CellPress

Matter

Perspective

Molecular Materials with Short Radiative Lifetime for High-Speed Light-Emitting Devices

Yingbo Zhao,[1,2] Vivian Wang,[1,2] and Ali Javey[1,2,*]

SUMMARY

Optical communication and interconnects utilize high-speed light sources for information transmission. The modulation frequency of light-emitting devices operating through spontaneous emission is fundamentally limited by the material intrinsic radiative lifetime. In this perspective, we examine the radiative lifetime of different materials and identify the superradiant molecular J aggregates as a promising class of materials for high-speed light-emitting devices. These molecular aggregates are relatively unexplored for electroluminescent devices and can have short radiative lifetime on the order of 10 ps while maintaining high photoluminescence quantum yield. The relation between intermolecular interactions, molecular packing geometry, and radiative lifetimes is presented theoretically in the context of Frenkel excitons and is corroborated with experimental examples. We further demonstrate the potential of designing superradiant materials through molecular engineering. We believe that these superradiant molecular materials will open up new opportunities in the fabrication of efficient and high-speed light-emitting devices.

INTRODUCTION

Optical communications and interconnects rely on high-frequency modulation light sources for high-speed information transmission. The commonly used light sources include lasers and light-emitting diodes. Lasers can be modulated at high speed but require complex fabrication steps and are energy intensive. Light-emitting devices operating thorough spontaneous emission can have reduced fabrication complexity and energy consumption, and devices with modulation frequency above 1 GHz have been reported.[1,2] However, the speed of these devices is fundamentally limited by the spontaneous radiative lifetime of the light-emitting materials. Although the radiative lifetime can be reduced with well-designed cavities through the Purcell effect,[3,4] its implementation is material specific and introduces complications to device fabrication. Thus, developing materials with intrinsically short radiative lifetime is fundamental to increasing the speed of light-emitting devices. As the luminescent quantum yield is determined by the competition of radiative and non-radiative processes, materials with short radiative lifetime produce high modulation frequency while maintaining high electroluminescent quantum yields. For inorganic materials, their radiative lifetimes are generally determined by the crystal structures and can hardly be reduced below a few nanoseconds even with material engineering methods such as doping or downsizing. Molecular materials can have radiative lifetimes down to tens of picoseconds, which can be further reduced by molecular and crystal engineering. With favorable packing geometry, superradiance can be achieved in molecular aggregates where the radiative lifetime scales inversely with grain size. Thus, designing superradiant molecular crystals can lead to fundamental advancement in high-speed light-emitting devices.

Progress and Potential

Optical interconnects transmit signals between different parts of integrated circuits using light and have lower power consumption and latency than the conventional metal interconnects. The modulation frequency of the on-chip light sources in optical interconnects determines the signal transmission speed. In principle, on-chip lasers relying on stimulated emission can have high modulation frequency but also have high fabrication complexity and energy consumption. Thus, it is desirable to use light-emitting devices that operate through spontaneous emission as the on-chip light source. However, the operation speed of these devices is limited by the radiative lifetime of the emitting materials. In this perspective, we envision that elaborately designed fluorescence molecules can give rise to materials that have radiative lifetime shorter by several orders of magnitude than conventional inorganic semiconductors through a phenomenon termed superradiance.

CARRIER RECOMBINATION IN INORGANIC MATERIALS

In light-emitting devices, the generation of light takes place when electrons and holes recombine radiatively at a rate that depends on the radiative lifetime. For some inorganic semiconductors, the high dielectric constant largely screens the Coulomb attraction between the electrons and holes, which can thus move independently in the conduction and valence band at room temperature. The radiative lifetime of these free carriers depends on the radiative recombination coefficient and the carrier concentration, which are related to the material band structure and doping level. Direct band-gap III–V semiconductors with moderate doping levels typically have radiative lifetimes of 10–100 ns.[5–12] Although the radiative lifetime would decrease with doping, heavy doping can result in non-radiative recombination by introducing trap states and promoting Auger processes (Figure 1A). When the thermal energy of the electrons and holes are not enough to overcome their Coulomb attraction, they become bound electron-hole pairs and behave as neutral quasiparticles termed excitons. The excitons can be categorized by their radius, which is the distance between the bound electron and hole. In inorganic semiconductors, due to the screened Coulomb interaction and large orbital overlap between atoms, the excitons typically have radius larger than the size of a lattice unit cell and are categorized as Wannier-Mott excitons. The bound electrons and holes have lower energy than the free carriers (Figure 1B) in the conduction and valence band corresponding to their binding energy, which is on the order of 10 meV and can be increased by quantum confinement.[13,14] II–VI quantum dots are a class of materials that host Wannier-Mott excitons, and their radiative lifetime is on the order of 10 ns. Although their radiative lifetime can be reduced by decreasing the particle size,[13,15] below a certain size (~2 nm) the quantum dots become chemically unstable and defective. The excitons can also form trions (with charged carriers) or biexcitons (with another exciton), which can have different radiative and non-radiative lifetimes.[16,17] For II–VI quantum dots, the radiative lifetime for trions and biexcitons can be twice as short as for the excitons, but still on the order of several nanoseconds.

EXCITON DYNAMICS OF MOLECULAR MATERIALS

The photophysics of excitons in molecular materials can be understood in the context of molecular orbitals (Figures 1C and 1D).[18–20] An isolated molecule can be conceptually simplified as a two-level system with the two energy levels being the highest occupied molecular orbital (HOMO) and lowest unoccupied molecular orbital (LUMO, Figure 1D). A molecule at its ground state typically has a pair of electrons with opposite spin occupying the HOMO, which is a singlet state denoted S_0. With optical excitation, one electron in the HOMO can be excited into the LUMO without changing its spin. The resulting singlet excited state (S_1) is conceptually equivalent to having one electron in LUMO and one hole in HOMO. In molecular solids, these excitations correspond to Frenkel excitons where the electron and hole reside in the same molecule. The radiative lifetime of a molecule is determined by the transition rate between the two states, which is proportional to the transition dipole moment μ (Equation 1). Here ϕ_g and ϕ_e denote the molecular ground and excited state wavefunction, q is the elemental charge, $\vec{r}$ is the position operator, and k_r is the rate of radiative recombination and the inverse of radiative lifetime. For molecules in singlet excited states, the recombination between the electron and hole gives fluorescence, which has radiative lifetime on the order of 1–100 ns. Besides radiative decay, the singlet excited state can also relax to the triplet state through intersystem crossing, whereby the electron excited into the LUMO would change its spin so that its spin is the same as the electron remaining in the

[1]Electrical Engineering and Computer Sciences, University of California at Berkeley, Berkeley, CA 94720, USA

[2]Materials Sciences Division, Lawrence Berkeley National Laboratory, Berkeley, CA 94720, USA

*Correspondence: ajavey@eecs.berkeley.edu

https://doi.org/10.1016/j.matt.2020.09.009

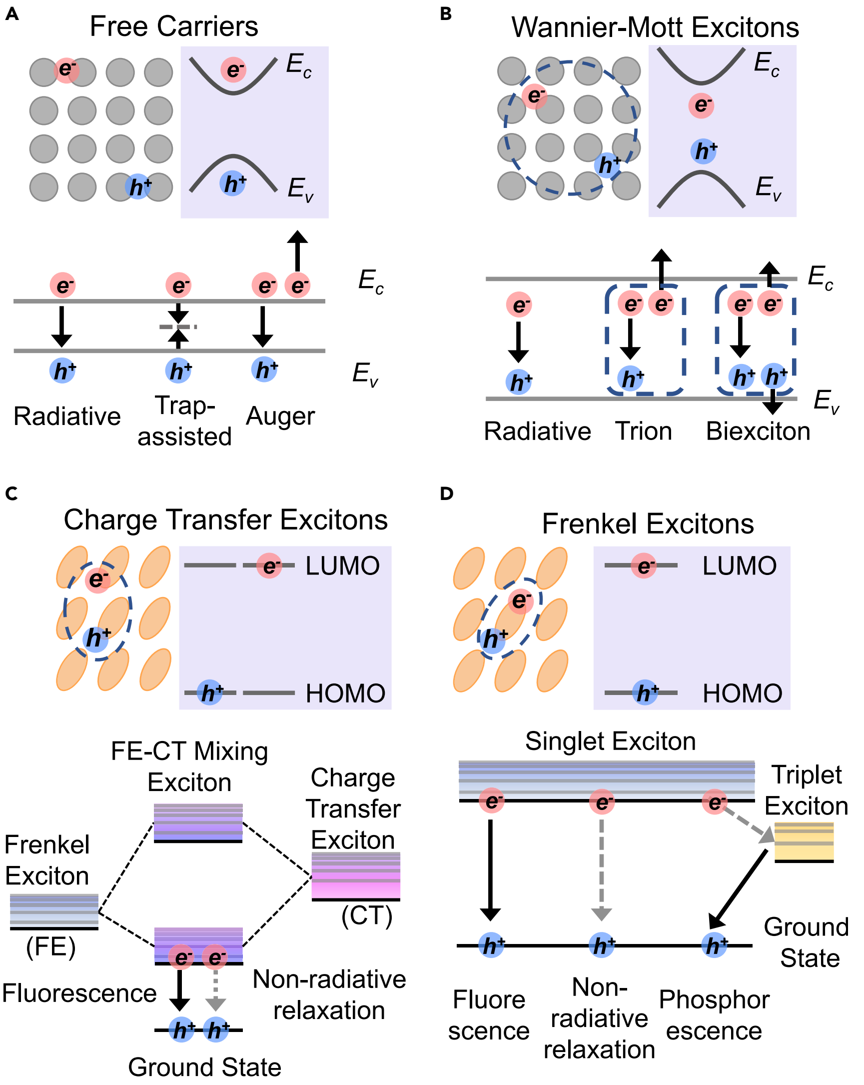

Figure 1. Dynamics of Carriers and Excitons in Different Materials

(A and B) (A) Electrons and holes can move freely in the electronic band of inorganic semiconductors (e.g., III–V compounds) as their Coulomb interaction is smaller than the thermal energy. The radiative band-to-band recombination of free carriers compete with the non-radiative trap-assisted and Auger recombinations. (B) The Wannier-Mott excitons can be described by a hydrogen-like model and have radius larger than several unit cells. Due to their binding energies, the electrons and holes have lower energy than the free carrier and thus are placed within the band gap.

(C) In molecular materials, an electron from the HOMO of a molecule can be excited into the LUMO of an adjacent molecule. Such excitation gives the charge-transfer exciton that has the electron and hole located on adjacent molecules. Charge-transfer excitons often mix with the Frenkel excitons and lead to red-shifted optical spectra due to the lowered exciton band energy.

(D) In a molecule, an electron from the HOMO can be excited to LUMO to produce a molecule in an excited state. The two unpaired electrons can have same or opposite spin, leading to triplet (T) or singlet (S) states. These molecular excitations lead to Frenkel excitons where the electron and holes are bound within the same molecule. Intermolecular interactions split the molecular excited states into exciton bands, where the radiative processes typically take place from the bottom of the exciton band to the ground state.

HOMO. Due to the spin-pairing energy, the triplet state would have a lower energy compared with the singlet state. The triplet state can decay to ground state via phosphorescence, which is spin forbidden and has radiative lifetime beyond hundreds of nanoseconds.

$$\vec{\mu} = \langle \phi_g | q\vec{r} | \phi_e \rangle \quad k_r = \frac{1}{\tau_{rad}} \propto \frac{4}{3}\frac{\nu^3}{\hbar c^3}|\vec{\mu}|^2 . \qquad \text{(Equation 1)}$$

The optoelectronic properties of molecular aggregates and crystals are different from isolated molecules due to the many-body Coulomb interactions between the electrons and nuclei of different molecules. When the intermolecular distance is significantly greater than the separation of charges within a molecule, Coulomb interaction can be approximated by the electrostatic interaction of electric dipoles. These materials host Frenkel excitons, which are molecular excitations delocalized in the material with each molecule having a certain possibility to be in the excited state. When the molecules are placed closer to each other, their molecular orbitals start to overlap. In these materials, the intermolecular interactions depend on the shape, phase, and orientation of the molecular orbitals of adjacent molecules and require quantum chemical treatment. The orbital overlap between nearby molecules facilitates charge transfer and delocalization. As a result, an electron from the HOMO of one molecule can be excited into the LUMO of other molecules in the material. This type of excitation gives charge-transfer excitons, which have the electron and hole bound to two different molecules. In actual molecular aggregates, although the intermolecular distance is comparable with the molecular size, the far field dipole approximation of Coulomb interaction is largely valid in materials without significant charge-transfer characteristics. For aromatic molecules with π conjugation, π-π stacking could lead to substantial orbital overlap between adjacent molecules; thus, charge-transfer excitons need to be considered when modeling their optical properties.

As the molecules have singlet and triplet excited states, Frenkel excitons in solids have singlet and triplet bands. Phosphorescence from the triplet band, similar to the phosphorescence from molecules, has long lifetime beyond 100 ns. Efficient phosphorescence typically involves heavy atoms that promote spin-orbit coupling.[21,22] The electron excited into the singlet band would first decay to the lowest energy state in the exciton band (internal conversion) before transition to the ground state via fluorescence,[23] which can have radiative lifetime down to nanoseconds. With increased wavefunction overlaps between the molecules, the charge-transfer exciton states can have energy low enough to mix with the Frenkel exciton and lower the energy of the first exciton band. Thus, these materials have red-shifted optical spectra, which are also broad due to the coupling to intermolecular vibrational modes.[18,19] Charge-transfer excitons tend to have longer radiative lifetime than Frenkel excitons due to larger separations of the electrons and holes.[24]

$$|k\rangle = \frac{1}{\sqrt{N}}\sum_n e^{ikn}|n\rangle \quad k = 0,\ \pm\frac{2\pi}{N},\ \ldots,\ \pi \quad |n\rangle = \phi_e^n \prod_{i\neq n}\phi_g^i , \qquad \text{(Equation 2)}$$

$$J = \frac{(3\cos^2\theta - 1)|\vec{\mu}|^2}{4\pi\varepsilon_0 R^3} \quad E_k = 2J\cos(k). \qquad \text{(Equation 3)}$$

PHOTOPHYSICS OF J AGGREGATES

The radiative lifetime of materials hosting Frenkel excitons can be shortened by engineering the molecular interactions, which can give rise to the superradiance phenomenon in molecular aggregates.[25,26] In this phenomenon, fluorescence from a

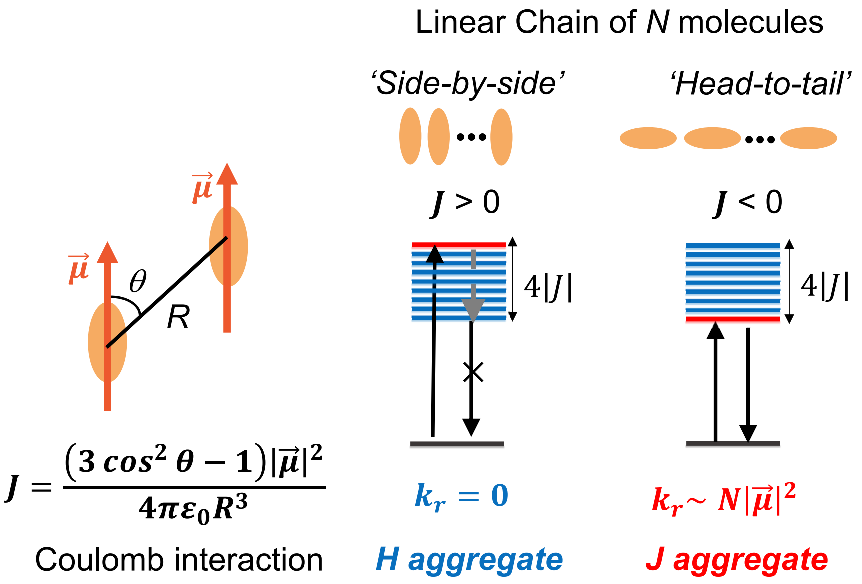

Figure 2. J and H Molecular Aggregates

For a linear chain of *N* molecules, the Coulomb interaction between the near-neighbors causes the splitting of single excited states into an exciton band. The molecular packing geometry determines the sign of Coulomb interaction, which determines whether the lowest energy level in the exciton band is optically allowed (J aggregates) or forbidden (H aggregates). The radiative lifetime of a J aggregate is *N* times lower than the monomer. J is the Coulomb energy between two molecules under the far field dipole approximation and $|k\rangle$ is the Frenkel exciton states defined in Equation 2. The orange oval denotes the molecule; the orange arrow denotes the molecular transition dipole moment.

certain exciton state can lead to radiative lifetime inversely proportional to the size of the aggregate. Molecular aggregates can be categorized as J and H aggregate depending on the sign of intermolecular Coulomb interactions. As a simple example, we describe the photophysics of molecular aggregates and the origin of superradiance with a linear chain of *N* molecules where the molecular transition dipole moments are parallel. With a far field dipole approximation, the effect of intermolecular interaction can be treated analytically and can lead to a simple relationship between molecular orientations and material radiative lifetimes. The ground state of the molecular chain is not affected by the intermolecular interactions and can be expressed as the multiplication of the molecular ground state wavefunctions. The excited states of the chain are linear combinations of the degenerate single-molecule excited states (Equation 2) in which the electrons and holes are bound within the same molecule.[18] Here, $|n>$ denotes the single-molecule excited states wavefunction where the *n*th molecule is in the excited state while all other molecules are in the ground state, and $|k>$ denotes the wavefunctions of the Frenkel excitons that form an exciton band. The radiative lifetime of the exciton can be related to the transition dipole moment after substituting the molecular electronic states with the exciton states. If we only consider the interaction between adjacent molecules, the energy of exciton states depends on the relative orientation between the molecular transition dipole and displacement vector connecting the molecular mass centers (Equations 2 and 3; Figure 2).[18] With negative Coulomb interaction energy, the all-symmetrical ($k = 0$) state has lowest energy in the exciton band, which is the state from which the radiative decay will occur. The transition dipole moment of this state is $\sqrt{N}$ times that of the molecular state, which gives the molecular aggregate *N* times shorter radiative lifetime as well as brighter fluorescence. In the classical picture in which

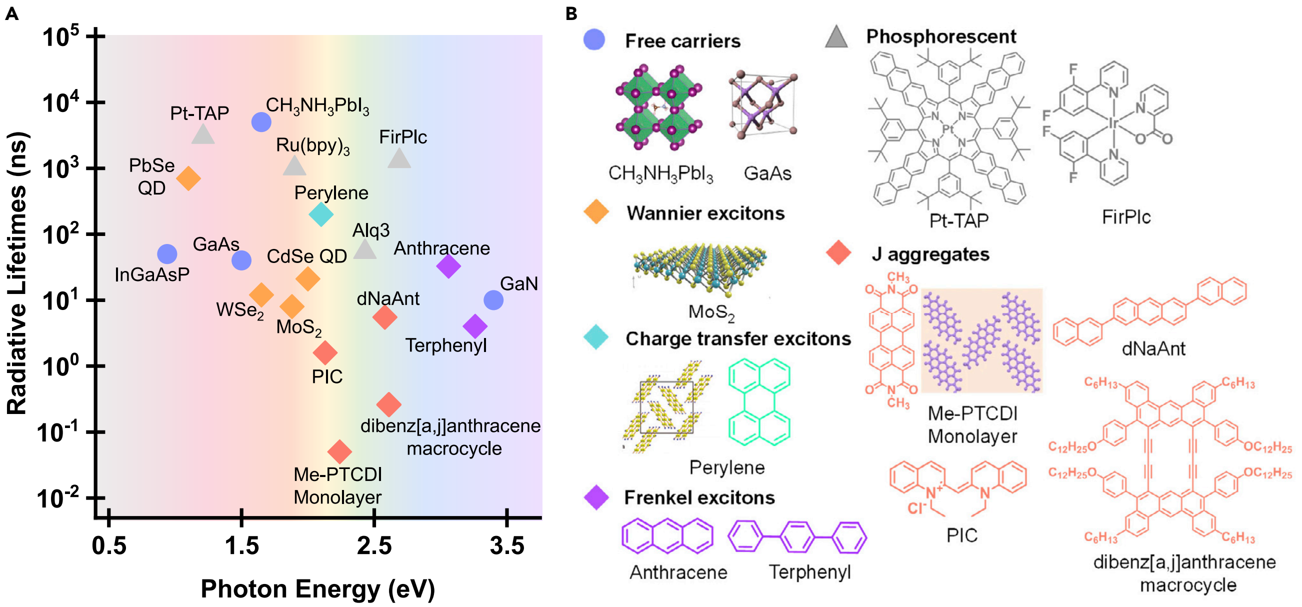

Figure 3. Radiative Lifetime of Materials with Different Mechanisms of Luminescence

The material lifetimes are summarized in (A) and their chemical structures and classification by type of excitons are listed in (B). The J aggregates also host Frenkel and charge-transfer excitons but are listed as a separate class to highlight their short radiative lifetimes.

the fluorescent molecules are treated as oscillating dipoles (the transition dipole), these dipoles in the molecular chain are aligned in the same direction into a giant oscillating dipole that has *N* times the oscillator strength of an isolated molecule. In actual molecular aggregates, due to the presence of disorder and the effect of finite temperature, the number of molecules that "coherently" interact with each other is often smaller than the size of the aggregates. In the absence of disorder, the coherence length is proportional to the square root of the Coulomb energy *J* divided by thermal energy *kT* (where *k* is Boltzmann's constant and *T* is temperature).[27] As the all-symmetrical state has lower energy than the molecular excited states, the optical spectra of the aggregate are red-shifted with respect to the isolated molecules. This type of molecular aggregate was discovered by Jelley and named as J aggregate.[28,29] Conversely, with positive Coulomb interaction energy, the all-symmetrical state is the highest energy state in the exciton band. The electron excited into this state would decay through internal conversion to the lowest energy state in the exciton band, which has zero transition dipole moment and thus a long radiative lifetime. In this case the aggregate is named H aggregate, as the absorption spectra have hypsochromic shift compared with the molecular monomer. With the existence of faster non-radiative decays, the H aggregate typically has weak fluorescence. Thus, the photophysics of molecular materials depends highly on the geometry of molecular assembly, which dictates the molecular interactions that determine material properties important to high-speed light-emitting devices.

RADIATIVE LIFETIME OF DIFFERENT MATERIALS

The lifetimes of a various fluorescent materials are summarized in Figure 3. The UV-emitting GaN has one of the shortest radiative lifetimes in materials hosting free carriers approaching 1 ns,[6,10] with the most widely used GaAs and InGaAsP having lifetime beyond 10 ns.[5,8] For lead iodide perovskite, although the direct band-gap material has radiative recombination coefficient similar to that of GaAs, its lower carrier concentration leads to the long radiative lifetime up to tens of microseconds.[30,31] The range of radiative lifetime of these free carrier materials corresponds to materials with different doping levels. Low-dimensional semiconductors hosting Wannier-Mott excitons such as quantum dots and transition metal dichalcogenides have radiative lifetime on the order of 10 ns.[15,32–35] As previously discussed, phosphorescent materials have long radiative lifetimes on the order of microseconds.[21,22] Among aromatic molecules, smaller molecules have larger optical band gap and weaker π stacking, and thus can host Frenkel excitons with radiative lifetime of a few nanoseconds.[36,37] With increasing conjugation size and without steric hindrance from side chains or functional groups, the tendency of π stacking between molecules increases, leading to a substantial portion of charge-transfer excitons and longer radiative lifetime of around 100 ns.[24] In general, extensive π stacking often leads to side-by-side packing geometry behaving as H aggregates, which is also undesirable for shortening the radiative lifetime. The pseudoisocyanine (PIC) molecular aggregates, where the J-aggregate behavior was first discovered, have radiative lifetime of 1.5 ns.[38] J-aggregate behavior can also be achieved in crystals of aromatic molecules, where some small molecules that host Frenkel excitons can directly crystallize into J aggregates (e.g., 2,6-diphenylanthracene).[39] For large conjugated molecules, bulky side chains can be used to reduce the charge-transfer exciton and facilitate the desirable molecular packing geometry.[40,41] Alternatively, the molecules can be assembled into ordered monolayers where the charge-transfer excitons can be greatly reduced and the intermolecular Coulomb interaction can lead to the formation of J aggregates.[42] The radiative lifetime of these materials can be reduced to tens of picoseconds,[42] corresponding to modulation frequencies on the order of sub-100 GHz for light-emitting devices, which is more than one order of magnitude faster than devices based on inorganic materials. We believe that molecular engineering and material design can produce J aggregates with lower radiative lifetime and enable light-emitting devices with modulation speed comparable with that of laser devices.

MATERIAL DESIGN FOR SUPERRADIANT J AGGREGATES

Although J aggregates were originally discovered in dye solutions by spectroscopic characterizations, the observation of the delocalized exciton states at submolecular level was made available in molecular aggregates adsorbed on single-crystalline substrates, which provides a rational route to the design of low-dimensional molecular J aggregates.[43] In this study, linear aggregates of ZnPc molecules were fabricated on a NaCl layer on single-crystalline silver substrate by a scanning tunneling microscopy (STM) tip under ultra-high vacuum (Figure 4). The tunneling current from the STM tip can excite the molecular aggregate to give fluorescence, which was used to map the spatial distribution of the transition dipole moment of the molecular aggregate at submolecular resolution. In the STM photon map, it was found that the fluorescence is strongest when the tip is located at the two ends of the linear aggregate, which is consistent with the transition dipole moment of the all-symmetrical excited state in the exciton band. This observation also validated the classical picture of J aggregates, in which the molecular transition dipole moments in the aggregate are aligned by the Coulomb interaction and produce a giant transition dipole moment that leads to a faster radiative decay rate proportional to the size of the aggregate. With an increased number of molecules in the aggregate, the tip-induced fluorescence spectrum progressively red-shifts and intensifies, accompanied by decreased effective fluorescence lifetime, which confirms the superradiant nature of J aggregates. This study demonstrated that molecules assembled laterally on substrate can form J aggregates that host Frenkel excitons. As the molecules assembled on the substrate as monolayers, there would be no intermolecular

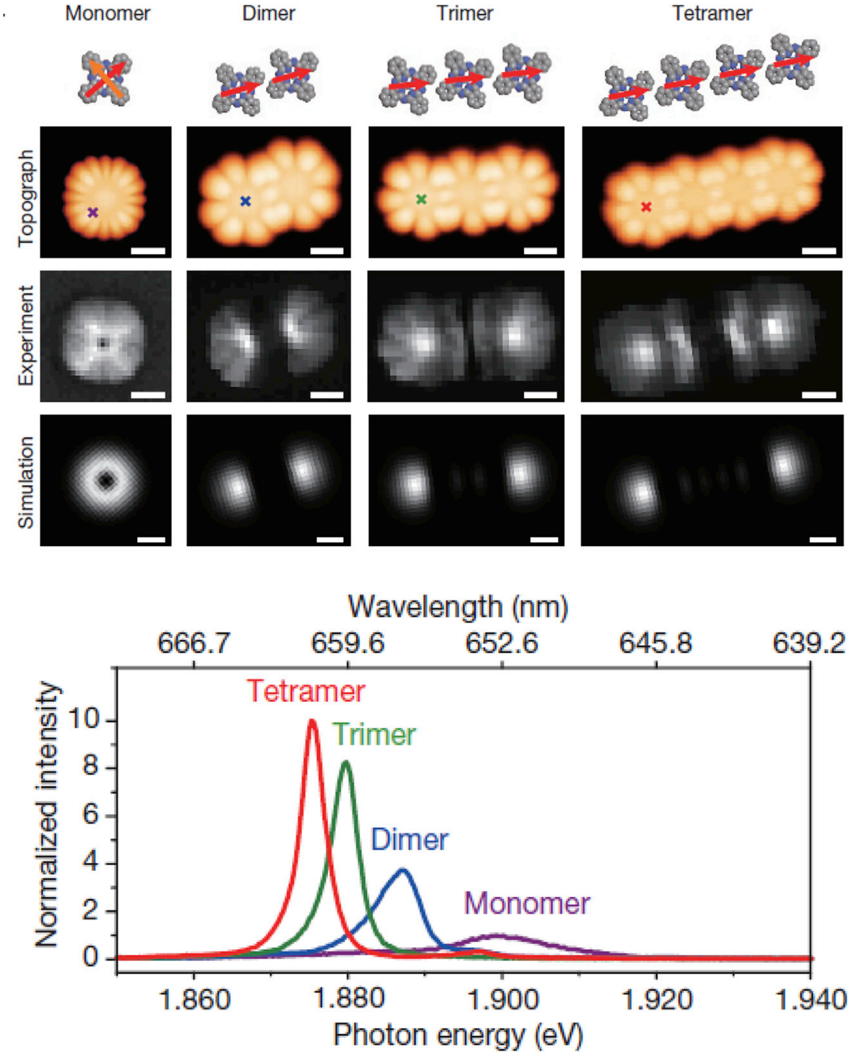

Figure 4. Superradiance of Artificially Fabricated Linear J Aggregates of ZnPc Studied by STM
The ZnPc molecules are absorbed on a NaCl layer on silver substrate, where the STM photon map visualized the transition dipole moment of the delocalized Frenkel exciton state. The fluorescence induced by tunneling current reached maximum when the tip was at the end of the aggregate, consistent with the giant transition dipole moment expected for J aggregates. The red-shifted and intensified fluorescence spectra with increased number of molecules are also characteristic of J aggregates. Adapted with permission from Zhang et al.[43] Copyright 2016, Springer Nature.

π stacking leading to charge-transfer excitons, which typically have longer lifetimes compared with the Frenkel excitons. Although the fabricated ZnPc molecular aggregates only have four molecules, the lateral assembly can in principle be extended to give two-dimensional molecular monolayers with low radiative lifetimes. With proper selection of the fluorescence molecule and substrate, these monolayers can be prepared using scalable methods, paving the way for high-speed light-emitting devices.

To achieve J-aggregate molecular monolayers that are stable under ambient condition and suitable for the fabrication of optoelectronic devices, several factors need to be considered for the selection of the molecules and substrate. First, the substrate needs to have atomically well-defined crystalline surfaces free from dangling bonds

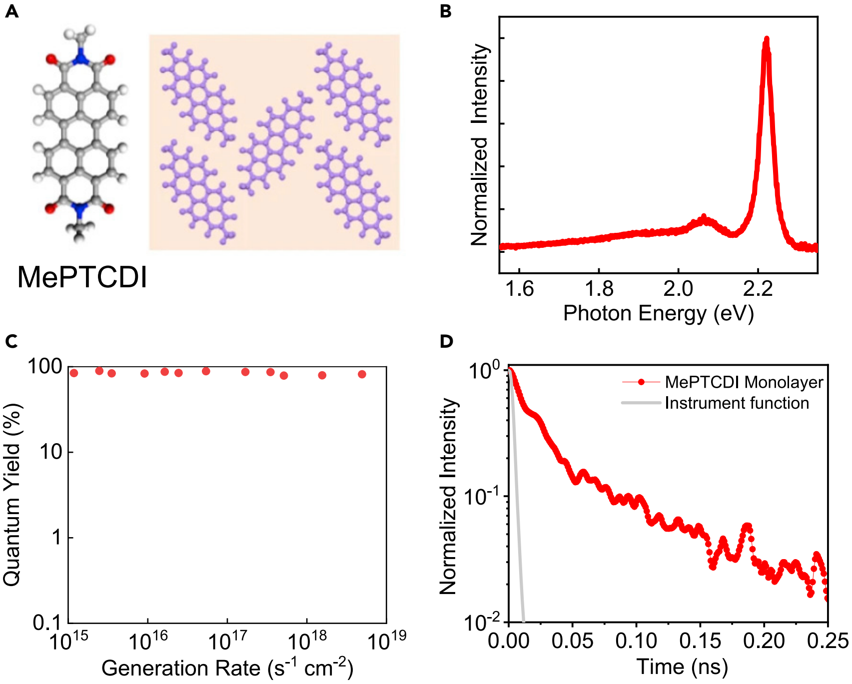

Figure 5. Photophysics of Me-PTCDI Monolayer

Me-PTCDI monolayer (A) on h-BN is a J aggregate hosting Frenkel excitons that combines narrow emission linewidth (B), high PLQY (C), and short radiative lifetime (D). Adapted with permission from Zhao et al.[42] Copyright 2019, Springer Nature.

to template the molecular assembly. Second, the molecules need to have strong interaction with the substrate to form a self-limited monolayer but cannot be quenched by the substrate. With these selection criteria, two-dimensional materials such as hexagonal boron nitride (h-BN) are the ideal choice for the substrate, which are atomically smooth and have large optical band gap that does not interfere with the fluorescence of the molecular layer. From numerous STM studies, it is known that ordered monolayers can be formed on these two-dimensional substrates with flat conjugated aromatic molecules such as perylene diimides,[44,45] which are also known to be optically active and have high photoluminescence quantum yield (PLQY) in isolated form. To this end, we prepared these perylene diimide monolayers on h-BN substrates and studied their optical properties (Figure 5).[42] We found that *N*,*N*′-dimethyl-3,4,9,10-perylenedicarboximide (Me-PTCDI) molecules form flat crystals with well-defined layer thickness corresponding to the π-π stacking distance. When the layer thickness is reduced to a monolayer, the charge-transfer excitons from π stacking between layers are removed, and the Frenkel excitons interact to form a J aggregate that simultaneously gives high PLQY, narrow emission linewidth, and short radiative lifetime of 27 ps. We believe that this method can be generalized to other aromatic molecules to achieve low-dimensional molecular crystals that have short radiative lifetime.

The molecular design of J aggregates with short radiative lifetime is not limited to molecular monolayers. Undesirable charge-transfer excitons can be removed from thicker molecular assemblies by isolating the core of the fluorescent molecules with side chains or reducing the π stacking with precisely designed molecular structures.[46] It has been shown that side chains added to perylene diimides effectively isolate the conjugated core of the molecule. Thin films of these molecules display

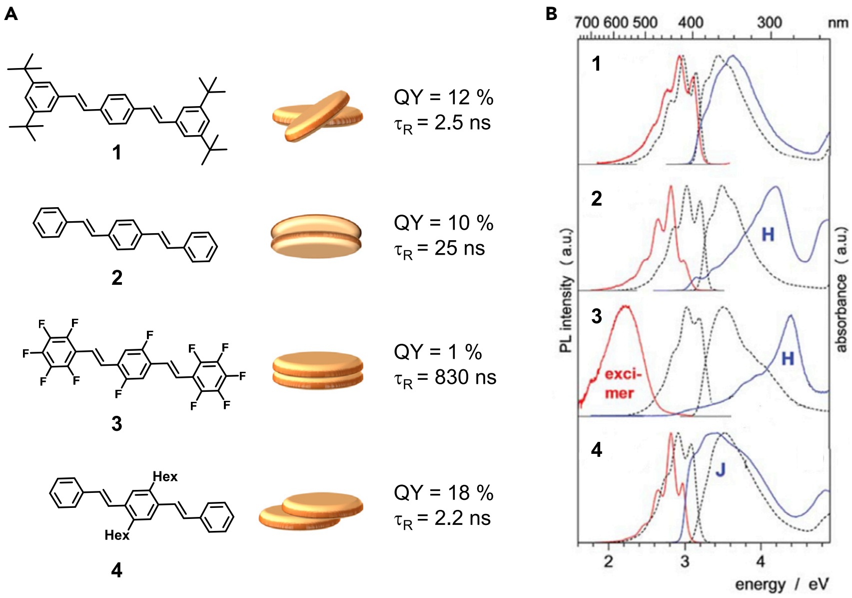

Figure 6. Molecular Engineering for J-Aggregate Behavior

Different substitutions on the *trans*-distyrylbenzene molecule give different packing structures (A) with different photoluminescence quantum yield (QY) and radiative lifetime (τ_R). The differences in their optical properties can be attributed to their J- and H-aggregate behavior and excimer band related to strong π stacking, which can be determined from their absorption and emission spectra (B). The dotted line is the absorption and emission spectra of the molecule in solution, which is similar among all four molecules. Adapted with permission from Gierschner et al.[47] Copyright 2013, The Royal Society of Chemistry.

higher photoluminescence quantum yield compared with that of the molecules without side chains and less red-shift in their solid-state fluorescence spectra, which both indicate the successful reduction of the charge-transfer excitons.[41] Another example demonstrating the versatility of molecular design is the distyrylbenzene derivatives, where different substitutions on the molecule change the packing of molecules from J to H aggregate and alter the degree of π stacking between molecules (Figure 6A).[47] Such differences in molecular packing have a direct impact on the radiative lifetime and optical spectra of the respective molecular materials. We believe that by properly selecting the molecular core and functionalization of molecular materials, J aggregates with simultaneously low radiative lifetime and high PLQY enable practical high-speed light-emitting devices for optical communication and interconnects.

HIGH-SPEED LIGHT-EMITTING DEVICES INCORPORATING J AGGREGATES

As superradiance in molecular materials relies on well-defined molecular packing geometries, rationally designed J aggregates would largely be crystalline materials that often form discontinuous films with pinholes. Low-dimensional J aggregates often need to be grown on flat, insulating substrates. Thus, conventional organic light-emitting diode structures that typically employ amorphous thin films are not suitable for crystalline J aggregates. AC-driven light-emitting devices have been reported to incorporate monolayer perylene diimides on h-BN where the h-BN substrate becomes part of the gate dielectrics (Figure 7A).[42] The AC-driven light-emitting devices with capacitor structures are also tolerant to pinholes and thus can incorporate low-dimensional or discontinuous materials. Electroluminescence

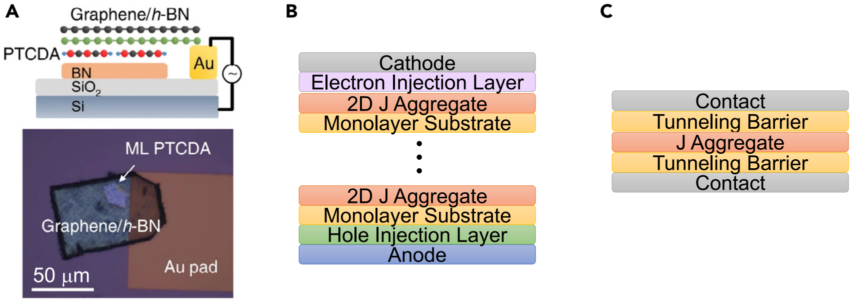

Figure 7. High-Speed Light-Emitting Devices Incorporating J Aggregates

(A) An AC-driven device with a capacitor structure can generate electroluminescence from perylene diimide molecular monolayers. Adapted with permission from Zhao et al.[42] Copyright 2019, Springer Nature.

(B) Proposed DC light-emitting devices adopting a structure similar to that of organic light-emitting diodes with charge-injection layers.

(C) Device structure operating with inelastic electron tunneling.

from these low-dimensional J aggregates can also be produced by inelastic electron tunneling, whereby the molecular layers are sandwiched between two insulating tunneling barriers and two electrodes (Figure 7B).[48] The device structure used for achieving electroluminescence from organic crystals could also be a promising candidate to incorporate J aggregates, and low-dimensional molecular layers can also be incorporated as a multilayer stack that is similar to multiple quantum well structure (Figure 7C)[49]. Light-emitting devices incorporating J aggregates can also employ cavities and antennas that further enhance the radiative recombination rate by the Purcell effect, which is a common device-designing strategy for high-speed light-emitting devices. The combination of intrinsic short radiative lifetime with enhancement from the cavity environment would give the light-emitting device with, ultimately, high operation speed.

CONCLUSION AND OUTLOOK

High-speed light-emitting devices are essential components of optical communications and interconnects, and their modulation frequencies are limited by the intrinsic radiative lifetimes of the light-emitting materials. While the intrinsic radiative lifetimes of inorganic materials are typically longer than 1 ns, some molecular materials (i.e., J aggregates) can have radiative lifetime down to 10 ps. In these materials, favorable molecular packing geometries lead to negative intermolecular Coulomb interaction energy that gives rise to superradiance, whereby the radiative lifetime of the material is inversely proportional to the number of molecules in the material. We believe that these molecular J aggregates are promising candidates for fabricating high-speed light-emitting devices due to their low radiative lifetime and high photoluminescence quantum yield. J aggregates can be designed by tuning the molecular packing geometry with molecular engineering methods such as attaching side chains or changing the functional groups. Low-dimensional J aggregates can be formed on atomically flat substrates which template their structures. We believe that with increased ability to predict the crystalline structure of molecules,[50,51] J aggregates with lower radiative lifetime can be developed. As J aggregates in solid state are often crystalline and form non-uniform films with pinholes, new device structures need to be designed to incorporate them in light-emitting devices. We believe that next-generation high-speed light-emitting devices would combine the short intrinsic radiative lifetime of J aggregates with Purcell effects enabled by optical antennas to produce operation frequencies beyond 100 GHz.

ACKNOWLEDGMENTS

The device design and characterization were funded by the NSF Center for Energy Efficient Electronics Science (E^{3}S). The materials characterization, including luminescence studies, were supported by the Electronic Materials Program, funded by the Director, Office of Science, Office of Basic Energy Sciences, Materials Sciences and Engineering Division of the US Department of Energy under contract no. DE-AC02-05Ch11231. V.W. acknowledges support from the NSF Graduate Research Fellowship (grant no. DGE-1752814).

AUTHOR CONTRIBUTIONS

Conceptualization, Y.Z. and A.J.; Validation, Y.Z., V.W., and A.J.; Writing – Original Draft, Y.Z.; Writing – Review & Editing V.W. and A.J.

REFERENCES

1. Koester, R., Sager, D., Quitsch, W.-A., Pfingsten, O., Poloczek, A., Blumenthal, S., Keller, G., Prost, W., Bacher, G., and Tegude, F.-J. (2015). High-speed GaN/GaInN nanowire array light-emitting diode on silicon(111). Nano Lett. *15*, 2318–2323.
2. Shi, J., Chi, K., Wun, J., Bowers, J., and Sheu, J. (2016). GaN based cyan light-emitting diodes with GHz bandwidth. In IEEE Photonics Conference (IPC 2016) (IEEE), pp. 623–624, https://doi.org/10.1109/IPCon.2016.7831257.
3. Noda, S., Fujita, M., and Asano, T. (2007). Spontaneous-emission control by photonic crystals and nanocavities. Nat. Photon. *1*, 449–458.
4. Fortuna, S.A., Heidelberger, C., Yablonovitch, E., Fitzgerald, E.A., and Wu, M.C. (2018). Nanoscale III-V light emitting diode with antenna-enhanced 250 picosecond spontaneous emission lifetime. In IEEE International Semiconductor Laser Conference (ISLC) (IEEE). https://doi.org/10.1109/ISLC.2018.8516244.
5. Henry, C., Levine, B., Logan, R., and Bethea, C. (1983). Minority carrier lifetime and luminescence efficiency of 1.3 μm InGaAsP-InP double heterostructure layers. IEEE J. Quan. Electron. *19*, 905–912.
6. Im, J.S., Moritz, A., Steuber, F., Härle, V., Scholz, F., and Hangleiter, A. (1997). Radiative carrier lifetime, momentum matrix element, and hole effective mass in GaN. Appl. Phys. Lett. *70*, 631–633.
7. Juršėnas, S., Miasojedovas, S., and Zukauskas, A. (2005). Rate of radiative and nonradiative recombination in bulk GaN grown by various techniques. J. Cryst. Growth *281*, 161–167.
8. Lush, G.B., MacMillan, H.F., Keyes, B.M., Levi, D.H., Melloch, M.R., Ahrenkiel, R.K., and Lundstrom, M.S. (1992). A study of minority carrier lifetime versus doping concentration in n-type GaAs grown by metalorganic chemical vapor deposition. J. Appl. Phys. *72*, 1436–1442.
9. Mickevičius, J., Shur, M.S., Fareed, R.S.Q., Zhang, J.P., Gaska, R., and Tamulaitis, G. (2005). Time-resolved experimental study of carrier lifetime in GaN epilayers. Appl. Phys. Lett. *87*, 241918.
10. Muth, J.F., Lee, J.H., Shmagin, I.K., Kolbas, R.M., Casey, H.C., Jr., Keller, B.P., Mishra, U.K., and DenBaars, S.P. (1997). Absorption coefficient, energy gap, exciton binding energy, and recombination lifetime of GaN obtained from transmission measurements. Appl. Phys. Lett. *71*, 2572–2574.
11. Semyonov, O., Subashiev, A., Chen, Z., and Luryi, S. (2010). Radiation efficiency of heavily doped bulk n-InP semiconductor. J. Appl. Phys. *108*, 013101.
12. Vilms, J., and Spicer, W.E. (1965). Quantum efficiency and radiative lifetime in p-type gallium arsenide. J. Appl. Phys. *36*, 2815–2821.
13. Elward, J.M., and Chakraborty, A. (2013). Effect of dot size on exciton binding energy and electron-hole recombination probability in CdSe quantum dots. J. Chem. Theor. Comput. *9*, 4351–4359.
14. Meulenberg, R.W., Lee, J.R.I., Wolcott, A., Zhang, J.Z., Terminello, L.J., and van Buuren, T. (2009). Determination of the exciton binding energy in CdSe quantum dots. ACS Nano *3*, 325–330.
15. Gong, K., Martin, J.E., Shea-Rohwer, L.E., Lu, P., and Kelley, D.F. (2015). Radiative lifetimes of zincblende CdSe/CdS quantum dots. J. Phys. Chem. C *119*, 2231–2238.
16. Sahin, M., and Koç, F. (2013). A model for the recombination and radiative lifetime of trions and biexcitons in spherically shaped semiconductor nanocrystals. Appl. Phys. Lett. *102*, 183103.
17. Jha, P.P., and Guyot-Sionnest, P. (2009). Trion decay in colloidal quantum dots. ACS Nano *3*, 1011–1015.
18. Hestand, N.J., and Spano, F.C. (2018). Expanded theory of H- and J-molecular aggregates: the effects of vibronic coupling and intermolecular charge transfer. Chem. Rev. *118*, 7069–7163.
19. Bardeen, C.J. (2014). The structure and dynamics of molecular excitons. Annu. Rev. Phys. Chem. *65*, 127–148.
20. Frenkel, J. (1931). On the transformation of light into heat in solids. Phys. Rev. *37*, 17–44.
21. Sommer, J.R., Shelton, A.H., Parthasarathy, A., Ghiviriga, I., Reynolds, J.R., and Schanze, K.S. (2011). Photophysical properties of near-infrared phosphorescent π-extended platinum porphyrins. Chem. Mater. *23*, 5296–5304.
22. Sarma, M., Tsai, W.-L., Lee, W.-K., Chi, Y., Wu, C.-C., Liu, S.-H., Chou, P.-T., and Wong, K.-T. (2017). Anomalously long-lasting blue PhOLED featuring phenyl-pyrimidine cyclometalated iridium emitter. Chem *3*, 461–476.
23. Kasha, M. (1950). Characterization of electronic transitions in complex molecules. Faraday Discuss *9*, 14–19.
24. Katoh, R., Suzuki, K., Furube, A., Kotani, M., and Tokumaru, K. (2009). Fluorescence quantum yield of aromatic hydrocarbon crystals. J. Phys. Chem. C *113*, 2961–2965.
25. Kasha, M., Rawls, H.R., and El-Bayoumi, M.A. (1965). The exciton model in molecular spectroscopy. Pure Appl. Chem. *11*, 371–392.
26. Spano, F.C., and Mukamel, S. (1989). Superradiance in molecular aggregates. J. Chem. Phys. *91*, 683–700.
27. Yamagata, H., and Spano, F.C. (2014). Strong photophysical similarities between conjugated polymers and J-aggregates. J. Phys. Chem. Lett. *5*, 622–632.
28. Jelley, E.E. (1936). Spectral absorption and fluorescence of dyes in the molecular state. Nature *138*, 1009–1010.
29. Bricks, J.L., Slominskii, Y.L., Panas, I.D., and Demchenko, A.P. (2017). Fluorescent J-aggregates of cyanine dyes: basic research and applications review. Methods Appl. Fluoresc. *6*, 012001.
30. Alarousu, E., El-Zohry, A.M., Yin, J., Zhumekenov, A.A., Yang, C., Alhabshi, E., Gereige, I., AlSaggaf, A., Malko, A.V., Bakr, O.M., et al. (2017). Ultralong radiative states in hybrid perovskite crystals: compositions for submillimeter diffusion lengths. J. Phys. Chem. Lett. *8*, 4386–4390.
31. Yamada, Y., Nakamura, T., Endo, M., Wakamiya, A., and Kanemitsu, Y. (2014). Photocarrier recombination dynamics in perovskite $CH_3NH_3PbI_3$ for solar cell applications. J. Am. Chem. Soc. *136*, 11610–11613.
32. Amani, M., Lien, D.H., Kiriya, D., Xiao, J., Azcatl, A., Noh, J., Madhvapathy, S.R., Addou, R.,

Santosh, K.C., Dubey, M., et al. (2015). Near-unity photoluminescence quantum yield in MoS_2. Science *350*, 1065.

33. Du, H., Chen, C., Krishnan, R., Krauss, T.D., Harbold, J.M., Wise, F.W., Thomas, M.G., and Silcox, J. (2002). Optical properties of colloidal PbSe nanocrystals. Nano Lett. *2*, 1321–1324.

34. Liu, H., and Guyot-Sionnest, P. (2010). Photoluminescence lifetime of lead selenide colloidal quantum dots. J. Phys. Chem. C *114*, 14860–14863.

35. Kim, H., Ahn, G.H., Cho, J., Amani, M., Mastandrea, J.P., Groschner, C.K., Lien, D.-H., Zhao, Y., Ager, J.W., Scott, M.C., et al. (2019). Synthetic WSe_2 monolayers with high photoluminescence quantum yield. Sci. Adv. *5*, eaau4728.

36. Horiguchi, R., Iwasaki, N., and Maruyama, Y. (1987). Time-resolved and temperature-dependent fluorescence spectra of anthracene and pyrene in crystalline and liquid states. J. Phys. Chem. *91*, 5135–5139.

37. Selvakumar, S., Sivaji, K., Arulchakkaravarthi, A., and Sankar, S. (2007). Enhanced fluorescence and time resolved fluorescence properties of p-terphenyl crystal grown by selective self seeded vertical Bridgman technique. Mater. Lett. *61*, 4718–4721.

38. Ermolaeva, G.M., Maslov, V.G., Orlova, A.O., Panfutova, A.S., Rosanov, N.N., Fainberg, B.D., Shakhverdov, T.A., and Shilov, V.B. (2011). Dynamics of optical response of solutions of pseudoisocyanine J aggregates upon pico- and subnanosecond excitation. Opt. Spectrosc. *110*, 871–879.

39. Li, J., Zhou, K., Liu, J., Zhen, Y., Liu, L., Zhang, J., Dong, H., Zhang, X., Jiang, L., and Hu, W. (2017). Aromatic extension at 2,6-positions of anthracene toward an elegant strategy for organic semiconductors with efficient charge transport and strong solid state emission. J. Am. Chem. Soc. *139*, 17261–17264.

40. Chan, J.M.W., Tischler, J.R., Kooi, S.E., Bulović, V., and Swager, T.M. (2009). Synthesis of J-aggregating dibenz[a,j]anthracene-based macrocycles. J. Am. Chem. Soc. *131*, 5659–5666.

41. Zhang, B., Soleimaninejad, H., Jones, D.J., White, J.M., Ghiggino, K.P., Smith, T.A., and Wong, W.W.H. (2017). Highly fluorescent molecularly insulated perylene diimides: effect of concentration on photophysical properties. Chem. Mater. *29*, 8395–8403.

42. Zhao, H., Zhao, Y., Song, Y., Zhou, M., Lv, W., Tao, L., Feng, Y., Song, B., Ma, Y., Zhang, J., et al. (2019). Strong optical response and light emission from a monolayer molecular crystal. Nat. Commun. *10*, 5589.

43. Zhang, Y., Luo, Y., Zhang, Y., Yu, Y.-J., Kuang, Y.-M., Zhang, L., Meng, Q.-S., Luo, Y., Yang, J.-L., Dong, Z.-C., and Hou, J.G. (2016). Visualizing coherent intermolecular dipole-dipole coupling in real space. Nature *531*, 623–627.

44. Emery, J.D., Wang, Q.H., Zarrouati, M., Fenter, P., Hersam, M.C., and Bedzyk, M.J. (2011). Structural analysis of PTCDA monolayers on epitaxial graphene with ultra-high vacuum scanning tunneling microscopy and high-resolution X-ray reflectivity. Surf. Sci. *605*, 1685–1693.

45. Kaneda, Y., Stawasz, M.E., Sampson, D.L., and Parkinson, B.A. (2001). STM investigations of the two-dimensional ordering of perylenetetracarboxylic acid N-alkyl-diimides on HOPG and MoS_2 surfaces. Langmuir *17*, 6185–6195.

46. Herbst, S., Soberats, B., Leowanawat, P., Stolte, M., Lehmann, M., and Würthner, F. (2018). Self-assembly of multi-stranded perylene dye J-aggregates in columnar liquid-crystalline phases. Nat. Commun. *9*, 2646.

47. Gierschner, J., and Park, S.Y. (2013). Luminescent distyrylbenzenes: tailoring molecular structure and crystalline morphology. J. Mater. Chem. C *1*, 5818–5832.

48. Svatek, S.A., Kerfoot, J., Summerfield, A., Nizovtsev, A.S., Korolkov, V.V., Taniguchi, T., Watanabe, K., Antolín, E., Besley, E., and Beton, P.H. (2020). Triplet excitation and electroluminescence from a supramolecular monolayer embedded in a boron nitride tunnel barrier. Nano Lett. *20*, 278–283.

49. Tischler, J.R., Bradley, M.S., Bulovic, V., Song, J.-H., Nurmikko, A., et al. (2005). Strong Coupling in a Microcavity LED. Phys. Rev. Lett. *95*, 036401.

50. Corpinot, M.K., and Bučar, D.-K. (2019). A practical guide to the design of molecular crystals. Cryst. Growth Des. *19*, 1426–1453.

51. Price, S.L. (2014). Predicting crystal structures of organic compounds. Chem. Soc. Rev. *43*, 2098–2111.